International Journal of Heat and Mass Transfer 51 (2008) 5949–5957

Contents lists available at ScienceDirect

International Journal of Heat and Mass Transfer

journal homepage: www.elsevier.com/locate/ijhmt

Fluid flow and heat transfer characteristics of natural convection in square cavities due to discrete source–sink pairs

Qi-Hong Deng *

School of Energy Science and Engineering, Central South University, Changsha, Hunan 410083, China

ARTICLE INFO

Article history:
Received 21 November 2007
Received in revised form 26 April 2008
Available online 1 July 2008

Keywords:
Natural convection
Discrete heat sources
Heat transfer enhancement
Optimal distribution
Heat transport
Heatlines

ABSTRACT

Laminar natural convection in a two-dimensional square cavity of side length H due to two and three discrete heat source–sink pairs on the vertical sidewalls was numerically investigated. Main efforts were focused on the size and arrangement effects of the sources and sinks on the fluid flow and heat transfer characteristics. The sizes of sources and sinks were, respectively, $H/4$ for two sources–sinks pairs and $H/6$ for three sources–sinks pairs. The arrangement of the sources and sinks changes from the separated to staggered modes, i.e., first separately located on two sidewalls, then alternately located on two sidewalls, and finally alternately located on one sidewall. The fluid flow, heat transfer, and heat transport characteristics were illustrated by streamlines, isotherms and averaged Nusselt number, and heatlines. It was found that the total heat transfer was closely related with the number of eddies in the enclosure. When the sources and sinks were split into smaller segments and/or arranged in a staggered mode, the number of eddies in the enclosure would increase and hence heat transfer was augmented.

1. Introduction

Natural convection in rectangular enclosures with discrete heat sources has received considerable attention in the recent years. One reason is for its various engineering applications, such as electronics cooling, food storage, and passive cooling of buildings. The other is its complex nature of the fluid flow and heat transfer characteristics due to discrete heat sources of different type, size, location and strength. To meet the increasing demand of engineering applications, main efforts have been focused on the approaches to enhance the heat transfer from the discrete heat sources and thus to decrease the hot-spot temperature in the enclosure.

The interest of the present work is related to the natural convection in rectangular enclosures due to flush-mounted discrete heat sources on the walls. A systematic review of the recent literatures on this topic found that the available studies could be categorized into three classes according to the number of the discrete heat sources and sinks. First, one source and one sink. It was found that both size and location of the discrete heat source had significant impact on natural convection heat transfer. The studies [1–3] numerically analyzed the heat transfer in rectangular cavities with one partially heated and the other partially cooled sidewalls. Saeid and Pop [4] examined a porous cavity with one partially heated and the other wholly cooled sidewalls. El-Refaee et al. [5] investigated an inclined cavity due to one wholly heated and the other partially cooled sidewalls. Poulikakos [6] and Ishihara et al. [7] studied enclosures with partially heated and cooled zones on a single sidewall. Second, one source and multiple sinks. Various heat sink configurations and their effects on the heat transfer from the discrete heat source have been extensively investigated. Natural convection in enclosures with localized heating from below and symmetrical cooling from sidewalls were studied in literatures [8–11]. Dalal and Das [12] studied the natural convection inside a rectangular cavity heated from below and cooled from other walls. Cheikh et al. [13] and Sezai and Mohamad [14] investigated rectangular enclosures heated from below and cooled from above for a variety of thermal boundary conditions at the sidewalls. Third, multiple sources and one sink. The configurations and/or distributions of the discrete heat sources are of course the main focus. The numerical studies [15–18] investigated the roles of the discrete heat sources of different location, type, size, and strength in the overall heat transfer across the enclosure. Bae and Hyun [19] examined the effect of the transient variation of one discrete heat source on the others in a rectangular enclosure. Tou and Zhang [20] carried out a numerical study of natural convection in a 3D enclosure with an array of discrete heaters. The effect of the separation distance between discrete heat sources on the overall heat transfer has been investigated [21–24], and it was found that the optimal distance was not the conventional equi-spaced arrangement but related to Rayleigh number and heat source dimension, as recently concluded by Da Silva et al. [25].

However, there are very few contributions to the natural convection in enclosures with multiple discrete heat sources and

* Tel.: +86 731 8877175.
E-mail address: qhdeng@csu.edu.cn

0017-9310/$ - see front matter © 2008 Elsevier Ltd. All rights reserved.
doi:10.1016/j.ijheatmasstransfer.2008.04.062

Nomenclature

g	gravity acceleration	*Greeks*	
H	height of enclosure	α	thermal diffusivity
n	outward normal direction	β	expansion coefficient
Nu	average Nusselt number	ν	kinematic viscosity
p, P	dimensional and dimensionless pressures	ρ	density
Pr	Prandtl number	θ	heat function
Ra	Rayleigh number	ψ	stream function
t, T	dimensional and dimensionless temperature	Δt	temperature scale
u, v	dimensional velocity components in x and y directions		
U, V	dimensionless velocity components in X and Y directions	*Subscripts*	
x, y	dimensional coordinates	h	hot
X, Y	dimensionless coordinates	c	cold

multiple sinks. Randriazanamparany et al. [26] present a numerical study of unsteady natural convection inside an air-filled square cavity, heated from two opposite sides and cooled from the other two sides. Banerjee et al. [27] studied a square cavity with two discrete heat sources flush-mounted on its bottom wall and two cold sidewalls. Ishihara et al. [28] and Li and Braun [29] studied a 3D rectangular enclosure with upper cooling and lower heating zones on two symmetrical sidewalls. Oosthuizen and Paul [30] numerically investigated a 3D rectangular enclosure with two square heated sections on the bottom and the cooled sidewalls. Above studies showed that the fluid flow was rather complicated, multi-cellular and unsteady. But in the present work, the author will illustrate that this may provide a good approach to enhance the heat transfer, as a recent review of the constructal theory by Da Silva et al. [31] that the design of multi-scale and non-uniformly distributed flow structures could increase the system's heat transfer.

In order to better understand and further discover the complicated heat transfer in enclosures with multiple sources and sinks, the concept of heat function and its contour lines, heatlines, are currently adopted to visualize the heat transport process induced by convection. Since it was first suggested and defined by Kimura and Bejan [32] in 1983, the visualization technique has attracted much attention and been used in many numerical studies, as recently reviewed by Costa [33]. Heatlines exhibit the convective heat transport process from a microscopic view, which is very different from the conventional Nusselt number that macroscopically describes the heat transfer rate. In other words, the former is a process but the latter is a state. Sometimes, we may be confused by the final state of heat transfer without the help of the heat transport process. As an example, Fig. 1 shows the natural convection in a 2D rectangular enclosure with four discrete elements of the same size centrally located on the surrounding walls, two sources of high temperature t_h and two sinks of low temperature t_c (also referred as two source–sink pairs). It is surprising to find that the heat from the left source is sent to the right sink and the heat from the bottom source to the top sink as indicated by the Nusselt number values. But for the transport, paths cannot be intersected with each other, we are now truly puzzled by the heat transfer result. Resorting to the heatlines, we get to know that the heat from the left source is in fact transported to the top sink, i.e., the first sink along the flow direction, not the right sink as indicated by the Nusselt number, and then the heat from the bottom source is in turn transported by the clockwise circulation to the top and right sinks. Obviously, heatlines provide an easy way and more meaningful approach to understand the complicated heat transfer process.

The objective of the present work is to numerically explore the fundamental fluid flow and heat transfer characteristics for natural convection in two-dimensional rectangular enclosures with multiple discrete source–sink pairs. Main attentions are focused on the significant effects of the size and location of both sources and sinks on the multi-cellular flow structure in the enclosures and hence overall heat transfer.

2. Numerical analysis

2.1. Physical model

The physical model under consideration is natural convection in square enclosures of side length H due to multiple source–sink pairs flush-mounted on the vertical sidewalls, as schematically shown in Fig. 2. The heat sources are maintained at a constant temperature t_h, higher than that of the sinks t_c ($t_c < t_h$). Other parts of the enclosures are all thermally insulated.

The size effect of the sources and sinks is first considered. Fig. 2a shows two source–sink pairs where the sizes of the sources and sinks are all kept the same as $H/4$, and Fig. 2b shows three source–sink pairs where the sizes of sources and sinks are decreased to $H/6$, keeping the total size of these sources and sinks as H. Then, the arrangement effect of the sources and sinks is investigated. As shown in Fig. 2, three cases are considered, i.e., case 1 where the sources and sinks are separately located on two sidewalls, case 2 where the sources and sinks are alternately located on two sidewalls, and case 3 where the sources and sinks are alternately located on one sidewall.

Both size and arrangement of the sources and sinks have great impact on the fluid flow structures in the enclosure as follows:

(1) *Case 1.* Only one eddy will be formed in the enclosure for both two and three source–sink pairs.
(2) *Case 2.* There will be two eddies in the enclosure for two source–sink pairs but three eddies for three source–sink pairs.
(3) *Case 3.* Four eddies for two source–sink pairs but six eddies for three source–sink pairs will be formed in the enclosure.

As expected, the flow pattern evolves from uni-cellular to multi-cellular structures when the layout of the sources and sinks changes from separated to staggered modes. Likewise, the flow structure will be broken up into more eddies if the discrete elements are split into smaller segments.

2.2. Mathematical model

2.2.1. Governing equations

The natural convection is considered to be steady and laminar, and Boussinesq approximation is employed to account for the ther-

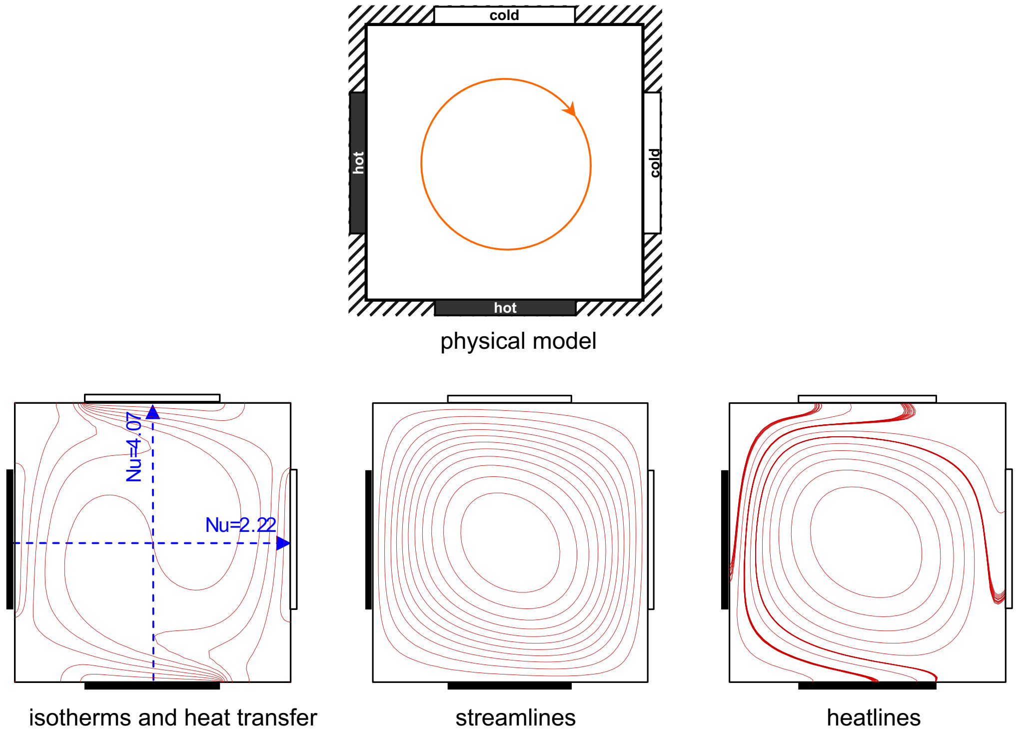

Fig. 1. An example to illustrate the difference between macroscopic heat transfer and microscopic heat transport for natural convection in square cavity with two source–sink pairs ($Ra = 10^5$).

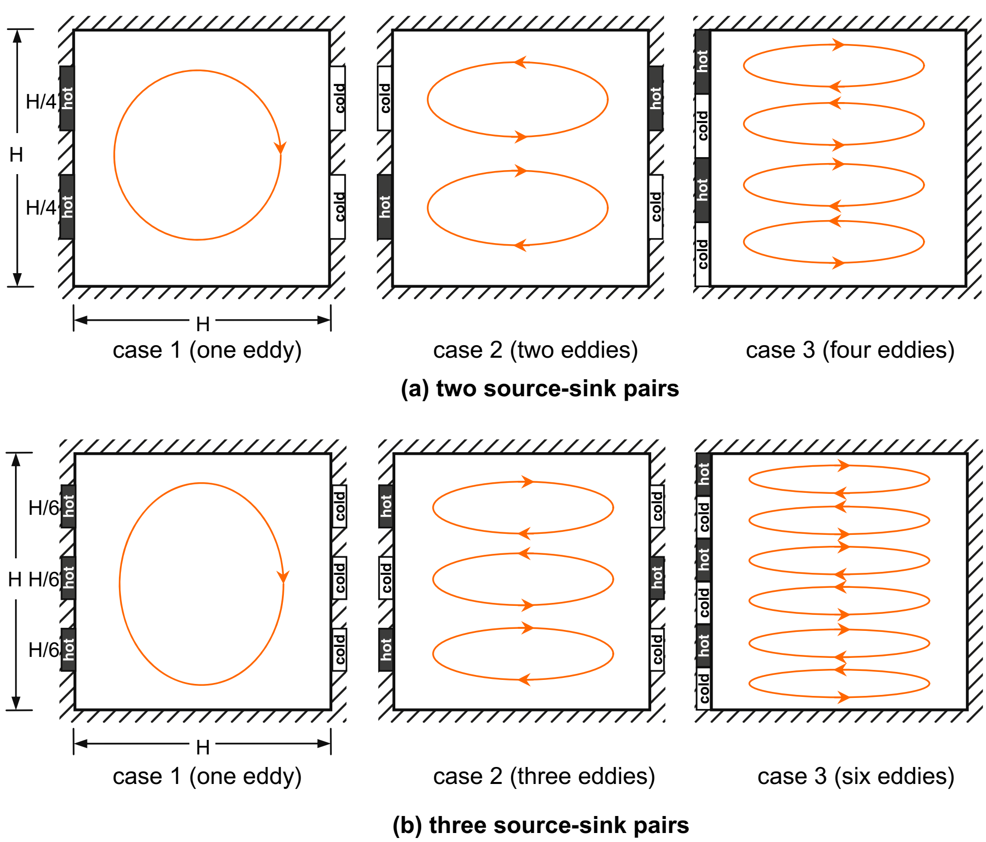

Fig. 2. Schematic of natural convection in square cavities with (a) two and (b) three source–sink pairs.

mal buoyancy effects. The governing equations in dimensionless form are as follows:

$$\frac{\partial U}{\partial X}+\frac{\partial V}{\partial Y}=0, \tag{1}$$

$$U\frac{\partial U}{\partial X}+V\frac{\partial U}{\partial Y}=-\frac{\partial P}{\partial X}+Pr\left(\frac{\partial^2 U}{\partial X^2}+\frac{\partial^2 U}{\partial Y^2}\right), \tag{2}$$

$$U\frac{\partial V}{\partial X}+V\frac{\partial V}{\partial Y}=-\frac{\partial P}{\partial Y}+Pr\left(\frac{\partial^2 V}{\partial X^2}+\frac{\partial^2 V}{\partial Y^2}\right)+RaPrT, \tag{3}$$

$$U\frac{\partial T}{\partial X}+V\frac{\partial T}{\partial Y}=\frac{\partial^2 T}{\partial X^2}+\frac{\partial^2 T}{\partial Y^2}. \tag{4}$$

The dimensionless variables in above equations are defined as $(X,Y) = (x,y)/H$, $(U,V) = (u,v)/(\alpha/H)$, $P = p/\rho(\alpha/H)^2$, and $T = (t-t_c)/\Delta t$ by using H, α/H, $\Delta t = t_h - t_c$ as characteristic scales for length, velocity, and temperature, respectively. The non-dimensional parameters, Rayleigh number and Prandtl number, are defined as

$$Ra = g\beta\Delta tH^3/\nu\alpha, \quad Pr = \nu/\alpha. \tag{5}$$

2.2.2. Boundary conditions

No-slip condition is imposed for all velocities on the walls. Thermal boundary conditions are, respectively, $T = 1$ for sources, $T = 0$ for sinks, and $\partial T/\partial n = 0$ for the insulated walls.

2.2.3. Stream function and heat function

The streamlines and heatlines are employed in the present work to visualize the fluid and heat transport processes. Stream function (ψ) are defined in terms of the continuity equation as

$$\frac{\partial\psi}{\partial Y}=U, \quad -\frac{\partial\psi}{\partial X}=V. \tag{6}$$

Heat function (θ) are defined in terms of the energy equation as

$$\frac{\partial\theta}{\partial Y}=UT-\frac{\partial T}{\partial X}, \quad -\frac{\partial\theta}{\partial X}=VT-\frac{\partial T}{\partial Y}. \tag{7}$$

2.2.4. Average Nusselt number

The heat transfer rate for each source or sink is described by the average Nusselt number which is defined as

$$Nu=\int_{\text{surface}}\left(-\frac{\partial T}{\partial X}\right)\mathrm{d}Y. \tag{8}$$

The total heat transfer rate across the whole cavity is the sum of the average Nusselt numbers over all sources or sinks.

2.2.5. Solution procedure

The governing equations, Eqs. (1)–(4), are discretized by the finite volume method (FVM) on non-uniform grid system [34]. The third-order QUICK scheme and the second-order central difference scheme are, respectively, implemented for the convection and diffusion terms. The set of discretized equations for each variable are solved by a line-by-line procedure, combining the tri-diagonal matrix algorithm (TDMA) with the successive over-relaxation iteration (SOR) method. The coupling between velocity and pressure is solved by SIMPLE algorithm [34]. The solution is terminated until the convergence criterion is reached, i.e., the maximal residual of all the governing equations is less than 10^{-6}. Then, the stream function (ψ) and heat function (θ) distributions within the calculation domain are obtained by using Eqs. (6) and (7), and the average Nusselt number on each source or sink and the total heat transfer rate across the whole cavity are obtained by using Eq. (8). The validity of the numerical method and code used in the present work has been confirmed in an earlier work about natural convection in rectangular enclosure with discrete heat sources [15].

3. Results and discussion

During the numerical calculation, the Prandtl number is kept constant as $Pr = 0.71$, but the Rayleigh number is varied within the laminar range, $Ra = 10^2$–10^6. Different arrangements of the sources and sinks and their effects on the fluid flow and heat transfer characteristics are first investigated for two and three source–sink pairs, respectively. Then, the size effect of the sources and sinks is studied by the comparison between the two and three source–sink pairs.

3.1. Two source–sink pairs

Fig. 3 showed the fluid flow and heat transfer characteristics and also heat transport structures by streamlines, isotherms, and heatlines for different arrangement of two source–sink pairs at $Ra = 10^6$. For case 1, the sources and sinks are separately located on two sidewalls, and their buoyancies are thus composed together, which creates only one eddy in the enclosure, i.e., the fluid is driven upward by the sources on the left sidewall and then downward by the sinks on the right sidewall. The average Nusselt number, as labeled in isotherms, macroscopically indicates the heat transfer relations between sources and sinks. It is found that the amount of heat released by the top source is equally absorbed by the bottom sink on the opposite sidewall ($Nu = 2.01$), and that the heat released by the bottom source is absorbed by the top sink on the opposite sidewall ($Nu = 4.05$). Heatlines, however, microscopically illustrate a different heat transport process. The heat picked up by the fluid from the top source on the left sidewall is not conveyed to the sink on the bottom but the one on the top of the right sidewall. On the other hand, the heat from the bottom source is conveyed by the fluid not only to the sink on the top but also the one on the bottom of the opposite sidewall. It is worth noting that heatline is also a visual measure of the heat transfer rate. Obviously, heatlines demonstrate that more heat is transferred from the bottom source than the top source, as indicated by the averaged Nusselt number ($Nu = 4.05 > 2.01$).

Because the sources and sinks are alternately located on two sidewalls for case 2, their buoyancies are decomposed into two groups, which generates two eddies, one counter-clockwise eddy set up by the source–sink pair in the upper region and the other clockwise eddy in the lower region, as shown by streamlines. The average Nusselt number illustrates that the heat transfer relation is such that the source corresponds with the sink on the same sidewall, as seen that the heat transfer rates are equal for bottom source and top sink both on the left sidewall and equal heat transfer rates for top source and bottom sink both on the right sidewall. However, heat transport process is quite different. Heatlines show that the heat from the top source is channeled by the upper counter-clockwise flow to the top sink on the opposite side. The heat from the bottom source is divided into two parts: one part is transported to the bottom sink on the opposite side by the lower clockwise flow, and the other part is transported to the top sink on the same side by the upper counter-clockwise flow. It is also obvious that more heat is transported from the bottom source than the top source, as indicated by the averaged Nusselt number ($Nu = 3.66 > 2.38$).

For the sources and sinks alternately locate on the same sidewall in case 3, their buoyancies are fully decomposed and therefore four eddies appear in the enclosure. The macroscopic heat transfer relation as revealed by the average Nusselt number is that the top source corresponds with the bottom sink ($Nu = 1.95$) and the bottom source reversely corresponds with the top sink ($Nu = 4.32$). But heatlines indicate that the heat from the top source is transported to only one sink along the flow direction. The heat from

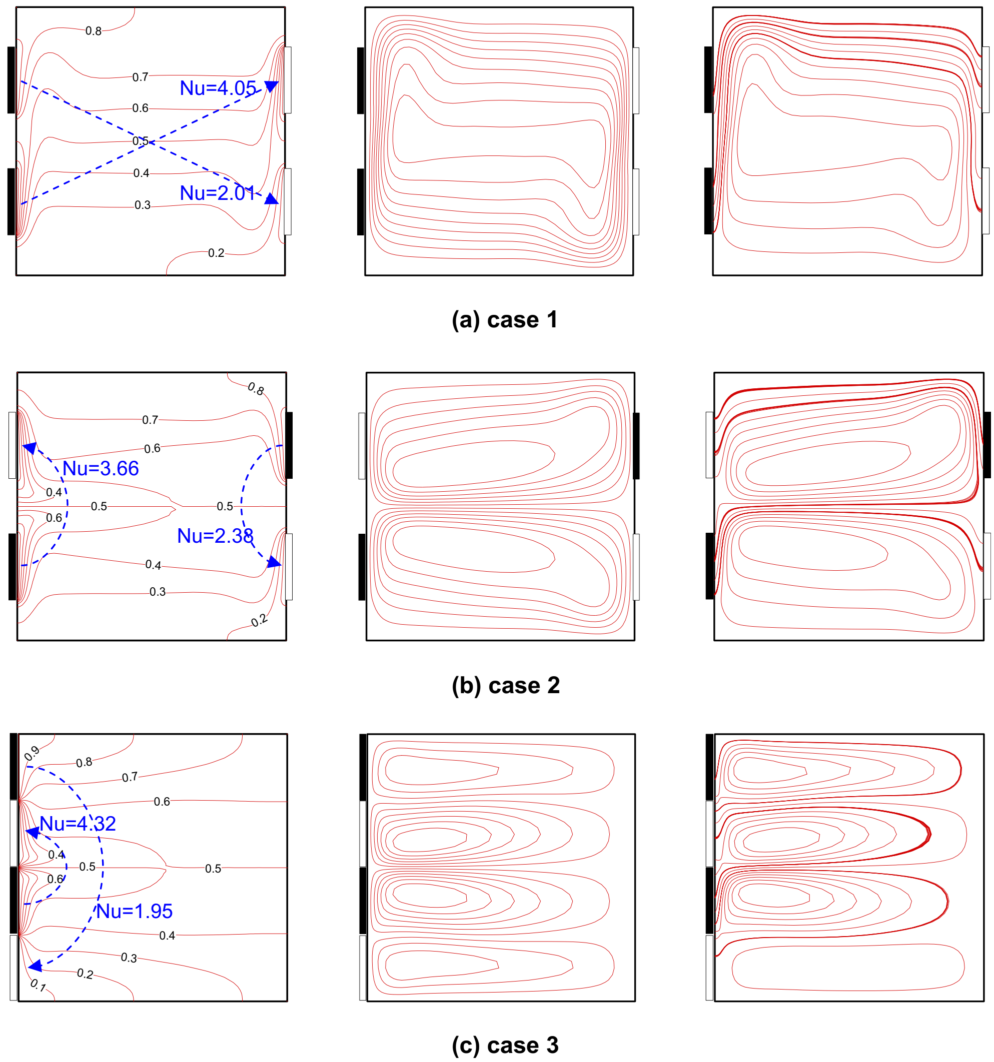

Fig. 3. Isotherms (left), streamlines (center), and heatlines (right) for different arrangement of two source–sink pairs at $Ra = 10^6$.

the bottom source is transported to two adjacent sinks in two directions, one towards the top sink by counter-clockwise flow and the other towards the bottom sink by clockwise flow. More heat is transported from the bottom source than the top source, as indicated by both heatlines and the averaged Nusselt number ($Nu = 4.32 > 1.95$).

From above three cases, one could obtain the following common heat transfer and heat transport characteristics. First, the average Nusselt numbers macroscopically illustrate that the heat transfer relation between sources and sinks is one (source) to one (sink) in a reversed manner, i.e., the top source corresponds with the bottom sink and the bottom source corresponds with the top sink. Second, the microscopic heat transport process is in a different manner and is determined by the fluid flow pattern. The heat from the top source can be only transported to one sink (top sink) along the flow direction, but the heat from the bottom source is transported to two sinks (both top and bottom sinks). Third, both macroscopic heat transfer and microscopic heat transport process indicate that the heat transfer rate from the lower source is always larger that that from the upper source.

Revisiting the isotherms, we can find that the fluid is thermally stratified when there is only one eddy in the enclosure (case 1). As two eddies appear (case 2), the downward cold fluid is mixed with the upward hot fluid, and the strong heat transfer between two streams causes the fluid in the center core of the enclosure is almost of average temperature. When there are four eddies in the enclosure (case 3), the vertical thermal stratification is almost destroyed, as seen that the center core region where the fluid is of uniform temperature is expanded due to more stronger mixing and heat transfer between four eddies than two eddies. Therefore, as the number of eddies in the enclosure increases, more and more fluid would be mixed, and thus the temperature of the fluid would be more uniform.

Fig. 4 plots the variations of total heat transfer from the sources or sinks in terms of Rayleigh number. It is clear that the total heat transfer rate is enhanced as Rayleigh number increases, but the tendency is much affected by the arrangement of sources and sinks or by the number of eddies in the enclosure. The heat transfer rate is the highest for case 3 where four eddies are formed in the enclosure, then the second for case 2 with two eddies, and the lowest for case 1 with only one eddy. In short, the more the number of eddies, the stronger the heat transfer. The reason may be due to the fact that the thermal boundary layer along the sources and sinks would be destroyed by eddies. Another key feature of the *Nu*–*Ra* curves is that the variations of total heat transfer rate undergo two regimes, i.e., conduction and convection regimes. Heat transfer first remains constant as Rayleigh number increases during the conduction dominated regime, then increases significantly during the

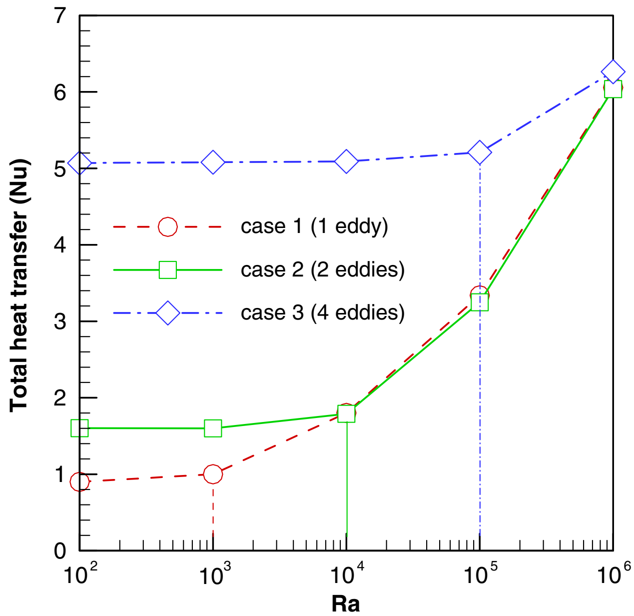

Fig. 4. Variations of total heat transfer rate with Rayleigh number (*Nu*–*Ra*) for different arrangement of two source–sink pairs.

convection regime. For case 1 with one eddy, the transition point from conduction to convection takes place early at $Ra = 10^3$. Due to the composed buoyancy effect of the sources and sinks, the fluid flow is strong and hence convection easily dominates the flow. The transition point is however postponed to $Ra = 10^4$ for case 2 with two eddies and further to $Ra = 10^5$ for case 3 with four eddies. This is due to the reason that the buoyancies of the sources and sinks are gradually decomposed, which makes the convection weaker and weaker and thus the conduction dominates the heat transfer mechanism longer and longer.

3.2. Three source–sink pairs

Fig. 5 shows the isotherms, streamlines, and heatlines for different layout of three source–sink pairs at $Ra = 10^6$. Similar to former case with two source–sink pairs, the composed buoyancies of the sources and sinks produce one eddy in the enclosure for case 1, and thus the fluid is evenly thermally stratified along the height of the enclosure. For case 2, the buoyancies of the sources and sinks are decomposed into three groups, which creates three eddies in the top, center, and bottom parts of the enclosure. The vertical thermal stratification is seriously destroyed, and the center core region of average temperature is enlarged as compared to the corresponding case of two source–sink pairs, Fig. 3b, due to the stronger mixing effect between three eddies than two eddies. As for case 3, the buoyancies of the sources and sinks are fully decomposed, which generates six eddies in the enclosure. Due to the strongest mixing and heat transfer between such many eddies, the thermal stratification phenomenon now disappears and even the fluid in most of the enclosure is of average temperature.

The average Nusselt numbers, as labeled in the isotherms of Fig. 5, demonstrate that the heat transfer relationship between three source–sink pairs is also “one to one” in a reversed manner, as found that the heat transfer rates from the bottom, center, and top sources are respectively equal to those from the top, center, and bottom sinks. Heat transport process is different from the final state of heat transfer, as observed by heatlines that (1) heat from the bottom source is transported to both bottom and center sinks, but cannot be transported to the top sink, (2) heat from the center source is transported to both center and top sinks, not just the center sink, and (3) heat from the top source is transported to top sink, not the bottom sink. Obviously, the heat transport is determined by the fluid flow pattern and the relationship between sources and sinks is not a “one to one” manner. However, the two approaches, both macroscopic and microscopic, consistently illustrate a larger heat transfer rate from the lower source than the upper source, such as $Nu = 3.04 > 2.44 > 1.08$ for case 1, $Nu = 2.54 > 2.16 > 1.48$ for case 2, and $Nu = 3.32 > 3.06 > 1.54$ for case 3.

The variations of total heat transfer rate in terms of Rayleigh number for above three cases are shown in Fig. 6. Similar to two source–sink pairs, some key features are found as follows: (1) the heat transfer is significant enhanced as the number of eddies in the enclosure increases, i.e., heat transfer is the highest for case 3 with six eddies, the second for case 2 with three eddies, and the lowest for case 1 with only one eddy; (2) the variations of total heat transfer rate undergo two stages, first remains constant as Rayleigh number increases during the conduction regime, but increases quickly during the convection regime; (3) the transition from conduction to convection is postponed as the eddies in the enclosure increase, as seen that the transition points are, respectively, $Ra = 10^3$ for case 1 with one eddy, $Ra = 10^4$ for case 2 with three eddies, and $Ra = 10^5$ for case 3 with six eddies.

3.3. Comparisons

Above heat transfer characteristics for two and three source–sink pairs are compared, as plotted in Fig. 7, which is combination of Fig. 4 and Fig. 6, so as to discover both size and arrangement effects of the sources and sinks or equivalently the number of eddies on the natural convective heat transfer in the enclosure. First, we keep the sizes of sources and sinks invariant and change their arrangements. The arrangement of sources and sinks changes from the separated to staggered modes, first separately located on two sidewalls (case 1), then alternately located on two sidewalls (case 2), and finally alternately located on the same sidewall (case 3). It has been proved that heat transfer increases as the flow structure evolves both from one eddy to three eddies to six eddies ($1 \rightarrow 3 \rightarrow 6$) for three source–sink pairs and from one eddy to two eddies to four eddies ($1 \rightarrow 2 \rightarrow 4$) for two source–sink pairs.

Second, we keep the arrangement of the sources and sinks invariant and change their sizes. The sizes of sources and sinks are decreased from the former $H/4$ for two sources-sinks pairs to the latter $H/6$ for three sources–sinks pairs. It is observed that the heat transfer nearly remains invariant as the flow structure is not seriously changed for case 1 with only one eddy, but the heat transfer is increased as the flow structure evolves both from two eddies to three eddies ($2 \rightarrow 3$) for case 2 and from four eddies to six eddies ($4 \rightarrow 6$) for case 3.

Combining above size and arrangement effects of the sources and sinks together, we could found that heat transfer is consistently enhanced as the number of eddies in the enclosure increases, i.e., the lowest for one eddy, then two eddies, three eddies, four eddies, and finally the highest for six eddies ($1 \rightarrow 2 \rightarrow 3 \rightarrow 4 \rightarrow 6$).

This means that the heat transfer in enclosures due to discrete sources and sinks could be maximized, only if we split the discrete elements into more and more smaller segments and then arrange them alternately in one sidewall so as to create the largest number of eddies in the enclosure.

It is worth noting that heat transfer is drastically enhanced and mainly dominated by conduction when the sources and sinks are placed in the most staggered order such as alternately located on the same sidewall (case 3). In order to find out the inherent reason, Fig. 8 shows the detailed isotherms, streamlines, and heatlines for $Ra = 10^3 \sim 10^6$. As discussed before, the buoyancies are now work-

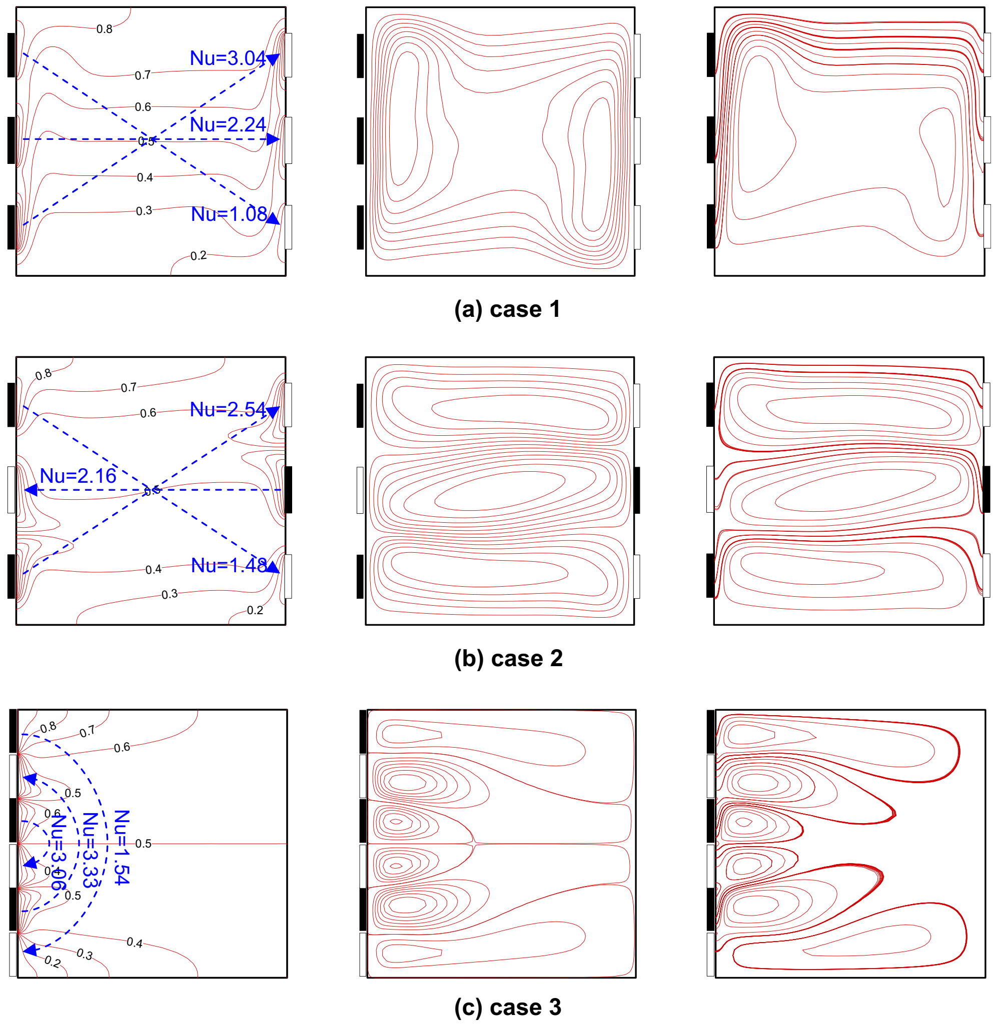

Fig. 5. Isotherms (left), streamlines (center), and heatlines (right) for different arrangement of three source–sink pairs at $Ra = 10^6$.

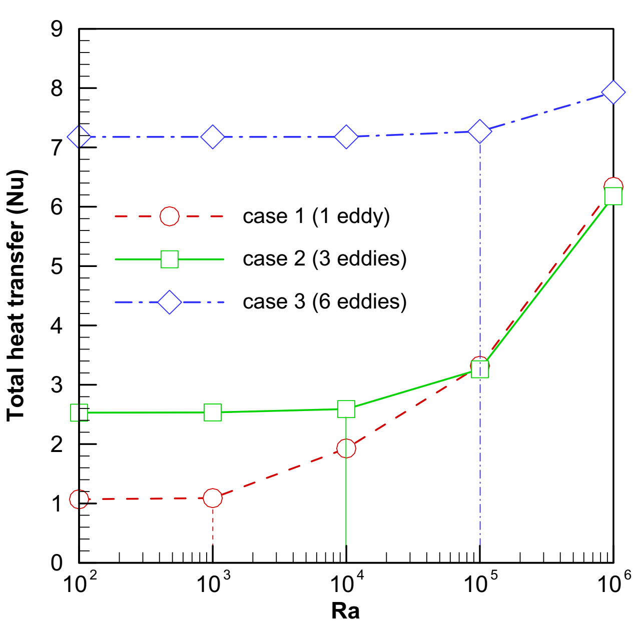

Fig. 6. Variations of total heat transfer rate with Rayleigh number (*Nu–Ra*) for different arrangement of three source–sink pairs.

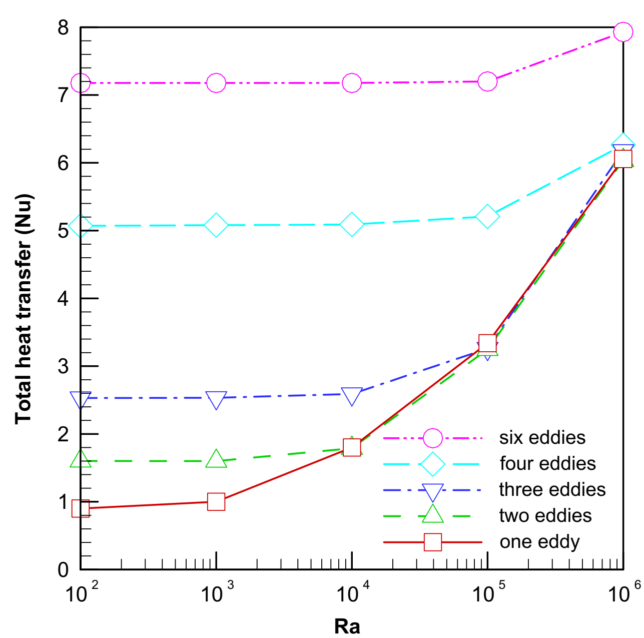

Fig. 7. Variations of total heat transfer rate with Rayleigh number (*Nu–Ra*) for different size and arrangement of source–sink pairs.

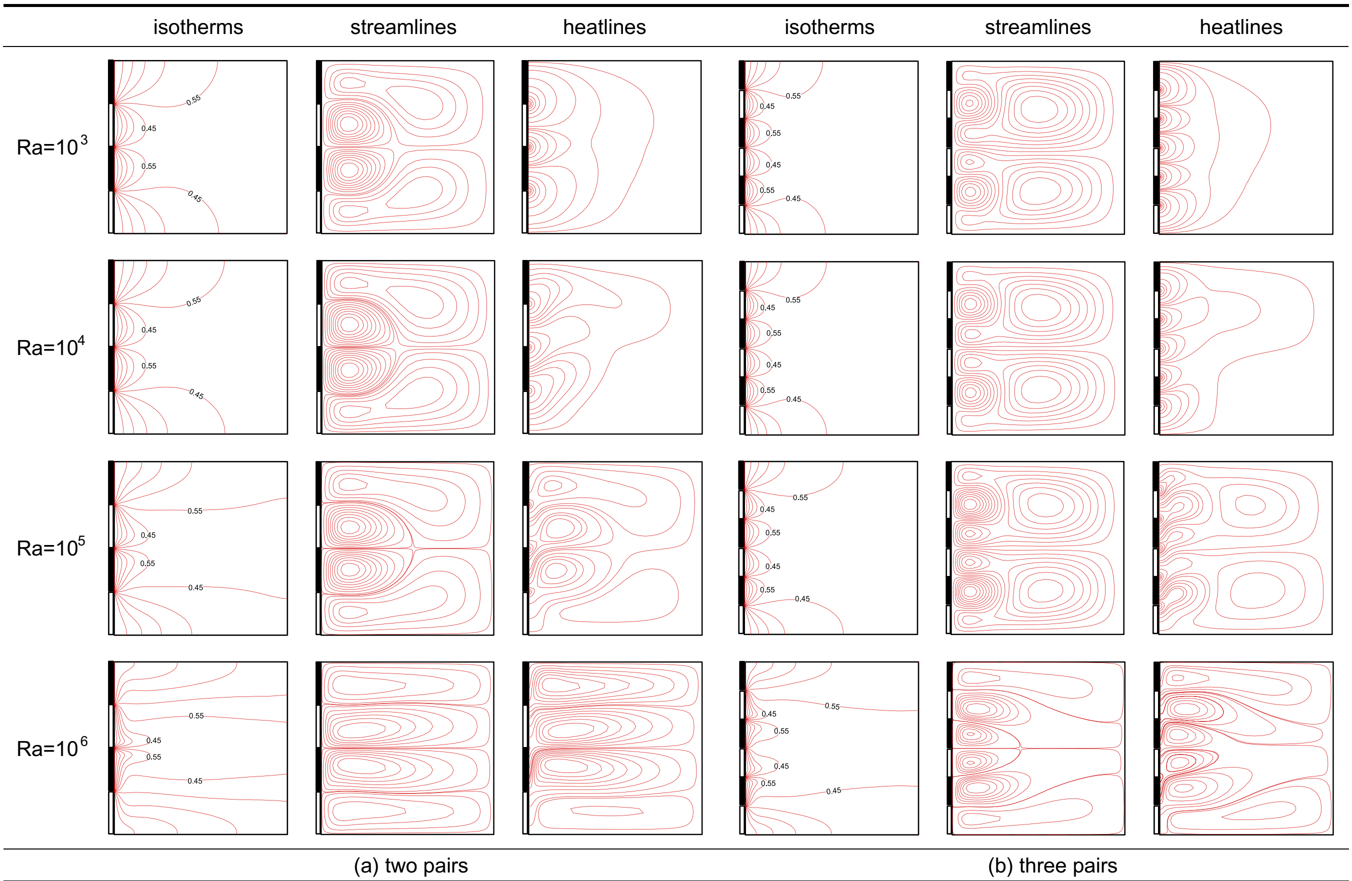

Fig. 8. Isotherms, streamlines, and heatlines for two and three source–sink pairs alternately arranged at the same side ($Ra = 10^3$–10^6). (a) Two pairs and (b) three pairs.

ing independently and generate the largest number of eddies in the enclosure. Due to fully mixing between eddies, the fluid in the region away from the sources and sinks is nearly of average temperature, and thus heat transfer occurs mainly within the thin region near to sources and sinks. It is observed that the convection is very weak at $Ra = 10^3$, as heatlines indicate that heat is essentially transferred by conduction mechanism. Obviously, the thermal penetration depth for two source–sink pairs is much larger than that for three source–sink pairs, and therefore heat transfer by conduction within the depth is substantially weaker for the former than the latter. As Rayleigh number increases, the convection is gradually strengthened, as seen that the heatlines are gradually affected by the flow pattern, and the thermal penetration depth is slowly increased. But heat transfer is still dominated by conduction mechanism and nearly remains invariant. Until $Ra = 10^6$, the convection prevails and thus heat transfer increases, as seen that eddies in the enclosure are fully developed and the thermal penetration depth is now extended to full length of the enclosure.

4. Conclusions

Laminar natural convection in a two-dimensional square enclosure due to two and three source–sink pairs on the vertical sidewalls was numerically investigated. Main efforts were focused on the size and arrangement effects of the sources and sinks on the fluid flow and heat transfer characteristics, and the following conclusions could be obtained.

The macroscopic heat transfer relationship between sources and sinks, in terms of the average Nusselt number values, is one to one in a reversed manner, i.e., the bottom source correspondences with the top sink and the top source correspondences with the bottom sink. The microscopic heat transport relationship is that the heat from the top source is transported to the only one (top) sink but the heat from the lower sources is transported to two adjacent sinks.

When the arrangement changes from the separated to staggered modes, the buoyancies of the sources and sinks are decomposed, the number of eddies in the enclosure increases and hence heat transfer increases. On the other hand, as the number of eddies increases, the strong mixing and heat transfer between eddies cause the temperature of the fluid in the enclosure more and more uniform.

When the sources and sinks are split into smaller segments (from $H/4$ to $H/6$), the number of sources and sinks increases (from two sources–sinks pairs to three sources–sinks pairs), which also increases the number of eddies in the enclosure, and therefore the heat transfer is increased.

Heat transfer is consistently enhanced as the number of eddies in the enclosure increases, i.e., the lowest for one eddy, then two eddies, three eddies, four eddies, and finally the highest for six eddies ($1 \to 2 \to 3 \to 4 \to 6$). This means that the heat transfer in enclosures due to discrete sources and sinks could be maximized if we split the sources and sinks into smaller segments and then place them in alternately on the same sidewall so as to create the largest number of eddies in the enclosure, but the optimal design approach need further investigation.

Acknowledgements

The work was financially supported by the following projects: National Natural Science Foundation of China (50408019), Foundation for the Author of National Excellent Doctoral Dissertation of PR China (FANEDD 200545), Program for New Century Excellent

Talents in University (NCET-05-0688), Fok Ying Tung Education Foundation (104006), Hunan Provincial Natural Science Foundation of China (06JJ1001). The author wishes to express his sincere thanks to above grants.

References

[1] N. Yücel, Natural convection in rectangular enclosures with partial heating and cooling, Heat Mass Transfer 29 (1994) 471–477.
[2] H. Türkoglu, N. Yücel, Effect of heater and cooler locations on natural convection in square cavities, Numer. Heat Transfer A 27 (1995) 351–358.
[3] N. Nithyadevi, N.P. Kandaswamy, J. Lee, Natural convection in a rectangular cavity with partially active side walls, Int. J. Heat Mass Transfer 50 (2007) 4688–4697.
[4] N.H. Saeid, I. Pop, Maximum density effects on natural convection from a discrete heater in a cavity filled with a porous medium, Acta Mechanica 171 (2004) 203–212.
[5] M.M. El-Refaee, M.M. Elsayed, N.M. Al-Najem, A.A. Noor, Natural convection in partially cooled tilted cavities, Int. J. Numer. Meth. Fluids 28 (1998) 477–499.
[6] P. Poulikakos, Natural convection in a confined fluid-filled space driven by a single vertical wall with warm and cold regions, ASME J. Heat Transfer 107 (1985) 867–876.
[7] I. Ishihara, R. Matsumoto, A. Senoo, Natural convection in a vertical rectangular enclosure with localizing heating and cooling zones, Heat Mass Transfer 36 (2000) 467–472.
[8] O. Aydin, W.J. Yang, Natural convection in enclosures with localized heating from below and symmetrical cooling from sides, Int. J. Numer. Meth. Heat Fluid Flow 10 (2000) 518–529.
[9] B. Calcagni, F. Marsili, M. Paroncini, Natural convective heat transfer in square enclosures heated from below, Appl. Therm. Eng. 25 (2005) 2522–2531.
[10] A.K. Sharma, K. Velusamy, C. Balaji, Turbulent natural convection in an enclosure with localized heating from below, Int. J. Therm. Sci. 46 (2007) 1232–1241.
[11] M.A.R. Sharif, T.R. Mohammad, Natural convection in cavities with constant flux heating at the bottom wall and isothermal cooling from the sidewalls, Int. J. Therm. Sci. 44 (2005) 865–878.
[12] A. Dalal, M.K. Das, Natural convection in a rectangular cavity heated from below and uniformly cooled from the top and both sides, Numer. Heat Transfer A 49 (2006) 301–322.
[13] N.B. Cheikh, B.B. Beya, T. Lili, Influence of thermal boundary conditions on natural convection in a square enclosure partially heated from below, Int. Commun. Heat Mass Transfer 34 (2007) 369–379.
[14] I. Sezai, A.A. Mohamad, Natural convection from a discrete heat source on the bottom of a horizontal enclosure, Int. J. Heat Mass Transfer 43 (2000) 2257–2266.
[15] Q.H. Deng, G.F. Tang, Y. Li, A combined temperature scale for analyzing natural convection in rectangular enclosures with discrete wall heat source, Int. J. Heat Mass Transfer 45 (2002) 3437–3446.
[16] Q.H. Deng, G.F. Tang, Y. Li, M.Y. Ha, Interaction between discrete heat sources in horizontal natural convection enclosures, Int. J. Heat Mass Transfer 45 (2002) 5117–5132.
[17] T.H. Chen, L.Y. Chen, Study of buoyancy-induced flows subjected to partially heated sources on the left and bottom walls in a square enclosure, Int. J. Therm. Sci. 46 (2007) 1219–1231.
[18] K. Ichimiya, H. Saiki, Behavior of thermal plumes from two-heat sources in an enclosure, Int. J. Heat Mass Transfer 48 (2005) 3461–3468.
[19] J.H. Bae, J.M. Hyun, Time-dependent buoyant convection in an enclosure with discrete heat sources, Int. J. Therm. Sci. 43 (2004) 3–11.
[20] S.K.W. Tou, X.F. Zhang, Three-dimensional numerical simulation of natural convection in an inclined liquid-filled enclosure with an array of discrete heaters, Int. J. Heat Mass Transfer 46 (2003) 127–138.
[21] A. Bazylak, N. Djilali, D. Sinton, Natural convection in an enclosure with distributed heat sources, Numer. Heat Transfer A 49 (2006) 655–667.
[22] Y. Liu, N. Phan-Thien, C.W. Leung, T.L. Chan, An optimum spacing problem for five chips on a horizontal substrate in a vertically insulated enclosure, Comput. Mech. 24 (1999) 310–318.
[23] Y. Liu, N. Phan-Thien, An optimum spacing problem for three chips mounted on a vertical substrate in an enclosure, Numer. Heat Transfer A 37 (2000) 613–630.
[24] J.T. Dias, L.F. Milanez, Optimal location of heat sources on a vertical wall with natural convection through genetic algorithms, Int. J. Heat Mass Transfer 49 (2006) 2090–2096.
[25] A.K. da Silva, S. Lorente, A. Bejan, Optimal distribution of discrete heat sources on a wall with natural convection, Int. J. Heat Mass Transfer 47 (2004) 203–214.
[26] M. Randriazanamparany, A. Skouta, M. Daguenet, Numerical study of the transition toward chaos of two-dimensional natural convection within a square cavity, Numer. Heat Transfer A 48 (2005) 127–147.
[27] S. Banerjee, A. Mukhopadhyay, S. Sen, R. Ganguly, Natural convection in a bi-heater configuration of passive electronic cooling, Int. J. Therm. Sci. 47 (2008), doi:10.1016/j.ijthermalsci.2007.12.004.
[28] I. Ishihara, T. Fukui, R. Matsumoto, Natural convection in a vertical rectangular enclosure with symmetrically localized heating and cooling zones, Int. J. Heat Fluid Flow 23 (2002) 366–372.
[29] H. Li, M.J. Braun, Flow structure and transport mechanism in lower half heated and upper half cooled enclosures in laminar flow regime, Heat Mass Transfer 42 (2006) 823–834.
[30] P.H. Oosthuizen, J.T. Paul, Natural convection in a rectangular enclosure with two heated sections on the lower surface, Int. J. Heat Fluid Flow 26 (2005) 587–596.
[31] A.K. da Silva, S. Lorente, A. Bejan, Constructal multi-scale structures for maximal heat transfer density, Energy 31 (2006) 620–635.
[32] S. Kimura, A. Bejan, The heatline visualization of convective heat transfer, ASME J. Heat Transfer 105 (1983) 916–919.
[33] V.A.F. Costa, Bejan's heatlines and masslines for convection visualization and analysis, ASME Appl. Mech. Rev. 59 (2006) 126–145.
[34] S.V. Patankar, Numerical Heat Transfer and Fluid Flow, Hemisphere, Washington, DC, 1980.